Journal of Industrial and Engineering Chemistry 16 (2010) 243–250

Contents lists available at ScienceDirect

Journal of Industrial and Engineering Chemistry

journal homepage: www.elsevier.com/locate/jiec

Synthesis of Y_2O_3 nano-powders by precipitation method using various precipitants and preparation of high stability dispersion for backlight unit (BLU)

Ji Yeon Jeong, Sun Woong Park, Doo Kyung Moon, Wha Jung Kim *

Department of Materials Chemistry and Engineering, College of Engineering, Kon Kuk University, 1-Hwa Yang Dong, Kwang Jin Gu, Seoul 143-701, Republic of Korea

ARTICLE INFO

Article history:
Received 23 July 2007
Accepted 25 November 2009

Keywords:
Precipitation
Precipitant
Effect of temperature
Transmittance
Brightness

ABSTRACT

Nano-sized yttria powder was successfully synthesized by precipitation method. Three different precipitants such as NH_4OH, mixture of NH_4OH and NH_4HCO_3, and NH_4HCO_3 were used. It was observed that the size of yttria powder is significantly affected by type of precipitant depending on the rate of formation of precipitate. It is seen that $NaHCO_3$ shows the most significant pH decrease during the formation of Y_2CO_3, thus leading to the formation of large crystal. The result also shows that the crystal size depends on calcinations temperature and the agglomeration have become more significant beyond 800 °C where the morphology have changed from flake to spherical shape interconnected each other. It was observed that the dispersity of yttria powder can be affected by bead size of ball mill, rpm and dispersion time where the physical, agglomeration has become more significant beyond 4 h of dispersion. Finally, the nano-sized yttria powder of on the average 114 nm shows excellent uniform coating, sufficient transmittance and excellent brightness for lamp.

1. Introduction

As conventional functional materials, rare earth metals and mostly their oxide compounds have been widely used in various fields, such as catalysts, fluorescence, laser applications, and electronic applications such as memory chips and superconductors [1–4]. In case of nano-sized rare earth oxides, their physical and chemical properties such as optical, electronic and catalytic properties are remarkably different from those of bulk materials. For this reasons, since the 1980s ultra fine rare earth oxides have been intensively studied. Among many rare earth oxides, zirconium, yttrium, titanium, and cerium are of particularly importance [5,6].

Yttria possesses excellent physical and chemical properties such as a high melting point (2698 K), high corrosion resistance and optical transparency over a wide wavelength range. Therefore, yttria has been widely used in many applications such as transparent ceramics, luminescent devices such as IR windows in heat seeking rockets and laser host materials [7–12].

Recently, the demand of liquid crystal display (LCD) has been rapidly grown and, moreover the backlight unit (BLU) market has become more important. The BLU is the most expensive part of LCD, and cold cathode fluorescent lamp (CCFL) as a main light source is especially regarded as one of the most important components in LCD. In addition, the length of the lamp used in BLU has been increased while its diameter has been reduced. As a consequence, it is critical to secure the dispersion technology of nano-sized powders such as yttria, zinc oxide or cesium sulfate to protect the inner surface of glass and phosphors in CCFL as well as to enhance the operating characteristics and life time of lamp.

The objectives of this study are to synthesize nano-sized yttria nano-powders using precipitation method and to provide the appropriate dispersion method of nano-sized yttria powder. Therefore, the effects of precipitant and calcination temperature on morphology, particle size, size distribution and agglomeration of yttria powders are discussed. Finally, the effects of organic solvent, dispersant and dispersion methods on the dispersity of nano-sized yttria powder and its application to cold cathode fluorescent lamp (CCFL) are also discussed.

2. Experimental

2.1. Materials

A series of experiments were conducted using different precipitants as follows. Yttrium(III) nitrate hexahydrate [$Y(NO_3)_3{\cdot}6H_2O$, 99.9%, Aldrich] was used as the starting material, and 2 M ammonium hydroxide solution [NH_4OH, Junsei], 0.9 M ammonium bicarbonate [NH_4HCO_3, 99.0%, SIGMA], and 0.9 M of the mixture of ammonia solution [NH_4OH, JUNSEI] and ammonium bicarbonate [NH_4HCO_3, 99.0%, SIGMA] in 1–1.1 molar ratio were used as precipitant, respectively.

* Corresponding author.
E-mail address: whajungk@konkuk.ac.kr (W.J. Kim).

1226-086X/$ – see front matter © 2010 The Korean Society of Industrial and Engineering Chemistry. Published by Elsevier B.V. All rights reserved.
doi:10.1016/j.jiec.2010.01.047

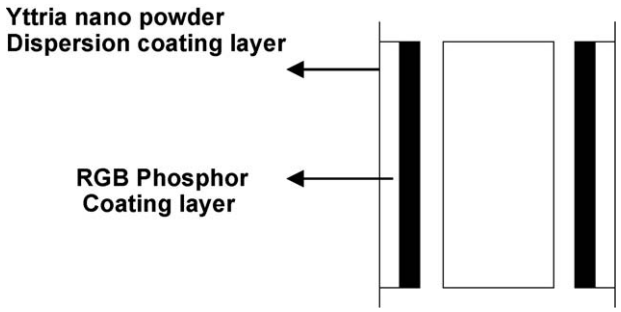

Fig. 1. Schematic diagram of CCFL.

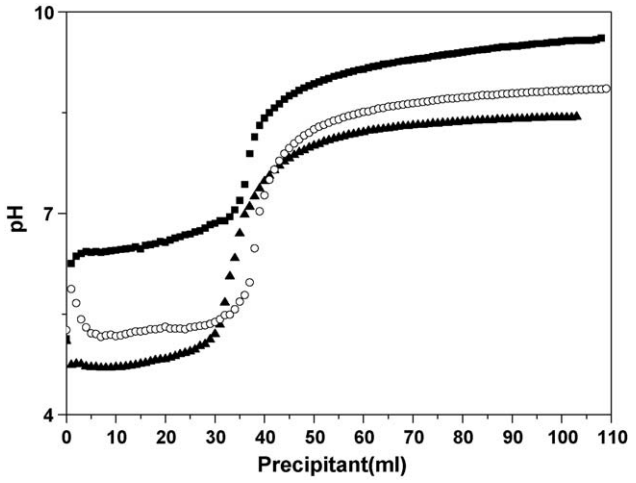

Fig. 2. pH variation of precursor metal salt solution with addition of precipitant; (■) 2 M NH_4OH, (○) mixture of 0.4 M NH_4OH and 0.44 M NH_4HCO_3, and (▲) NH_4HCO_3

2.2. Experimental procedures

In experiment set A, 0.26 M yttrium(III) nitrate hexahydrate [$Y(NO_3)_3{\cdot}6H_2O$] salt solution was prepared by dissolving salt in deionized water followed by 0.5 h of vigorous stirring at room temperature. After vigorous stirring, 2 M of ammonium hydroxide solution was slowly added to obtained salt solution. This solution was then pH adjusted and aged with mild agitation for various times at room temperature. The precipitates formed after aging were filtered and washed thoroughly with deionized water and dried overnight under air flow at 10 ml/min and 333 K. The obtained dry cake was ground in alumina mortar and pestle, followed by subsequent calcination at predetermined temperature under oxygen flow.

In experiment sets B and C, 0.9 M of the mixture of ammonium hydroxide and ammonium bicarbonate, and 0.9 M ammonium bicarbonate were slowly added to yttrium salt solutions, respectively, followed by the same procedures as described above.

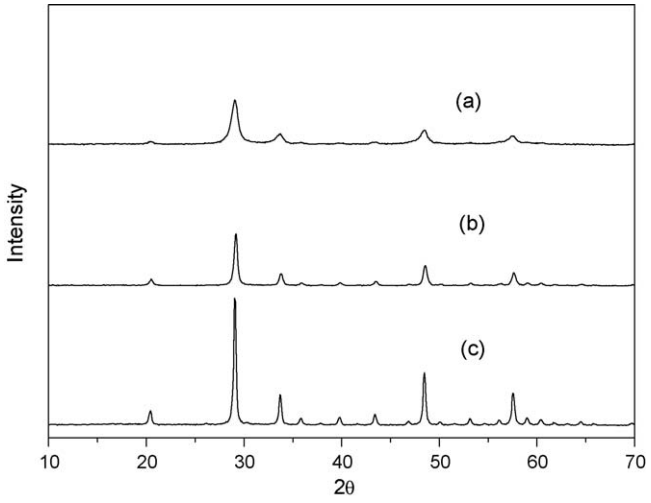

Fig. 3. XRD patterns of yttria powders synthesized using different precipitant; (a) NH_4OH solution, (b) $NH_4OH + NH_4HCO_3$ solution and (c) NH_4HCO_3 solution.

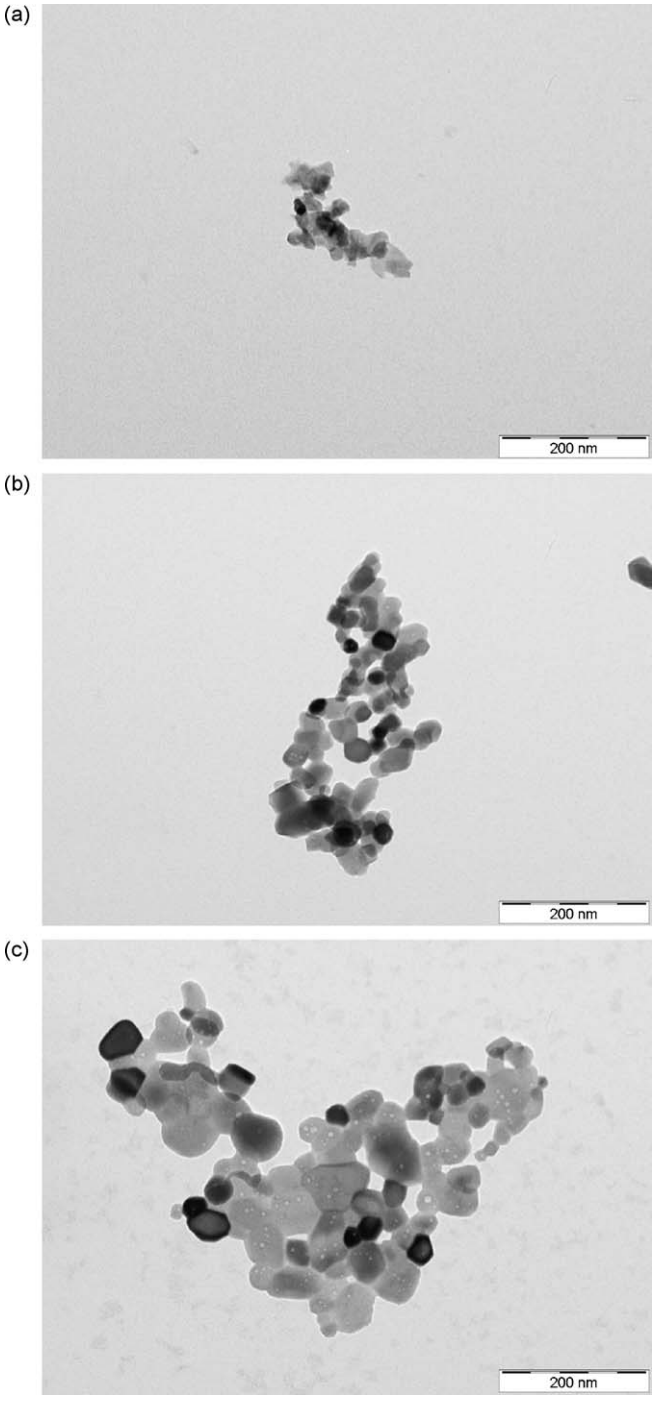

Fig. 4. FETEM of yttria powder samples after 4 h of calcinations at 800 °C synthesized at reaction time of 4 h and pH of 8; (a) NH_4OH solution, (b) $NH_4OH + NH_4HCO_3$ solution and (c) NH_4HCO_3 solution.

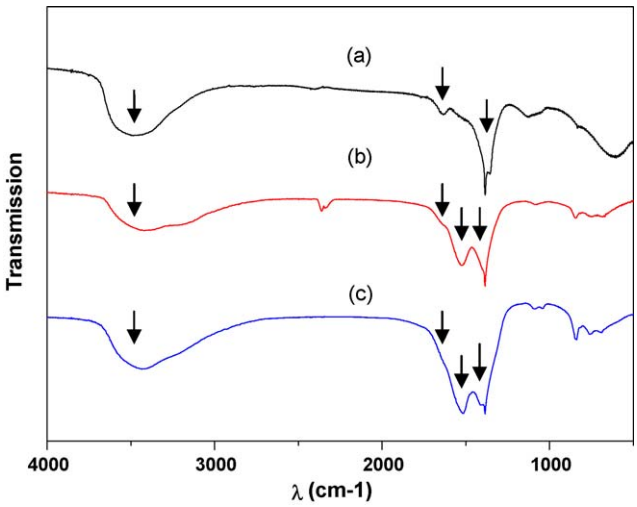

Fig. 5. IR spectra of the precursors prepared using different precipitants; (a) NH_4OH solution, (b) $NH_4OH + NH_4HCO_3$ solution and (c) NH_4HCO_3 solution.

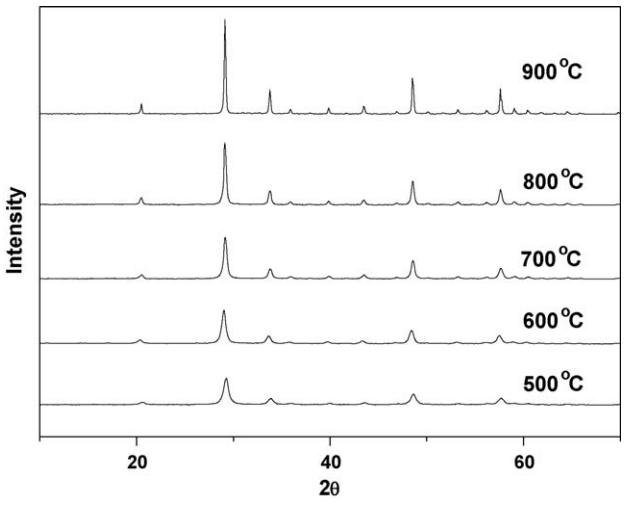

Fig. 6. XRD patterns of calcined yttria samples at different temperatures obtained at pH 7 and 4 h of aging at 40 °C.

As the first step of dispersion process, yttria nano-powder was dispersed in several organic solvents such as methyl ether ketone (MEK), normal butyl alcohol (NBA), ethyl acetate (EA) and isopropyl alcohol (IPA) to choose an optimal organic solvent showing the best dispersity. Once an optimal organic solvent was determined, to determine an optimal dispersant, yttria nano-powder was dispersed in several dispersants such as acrilate co-polymer, alkyl ammonium salt, and phosphoric acid ester.

Upon determining optimal organic solvent and dispersant, to prepare the coating solution for LED BLU, the yttria powder dispersed in dispersant was ball-milled using different size of bead with various rpm and dispersion time to optimize the experimental conditions. Based on the optimal conditions obtained, the nano-sized yttria dispersion was prepared and applied to CCFL as shown in Fig. 1. A schematic diagram of CCFL considered in this study is shown in Fig. 1.

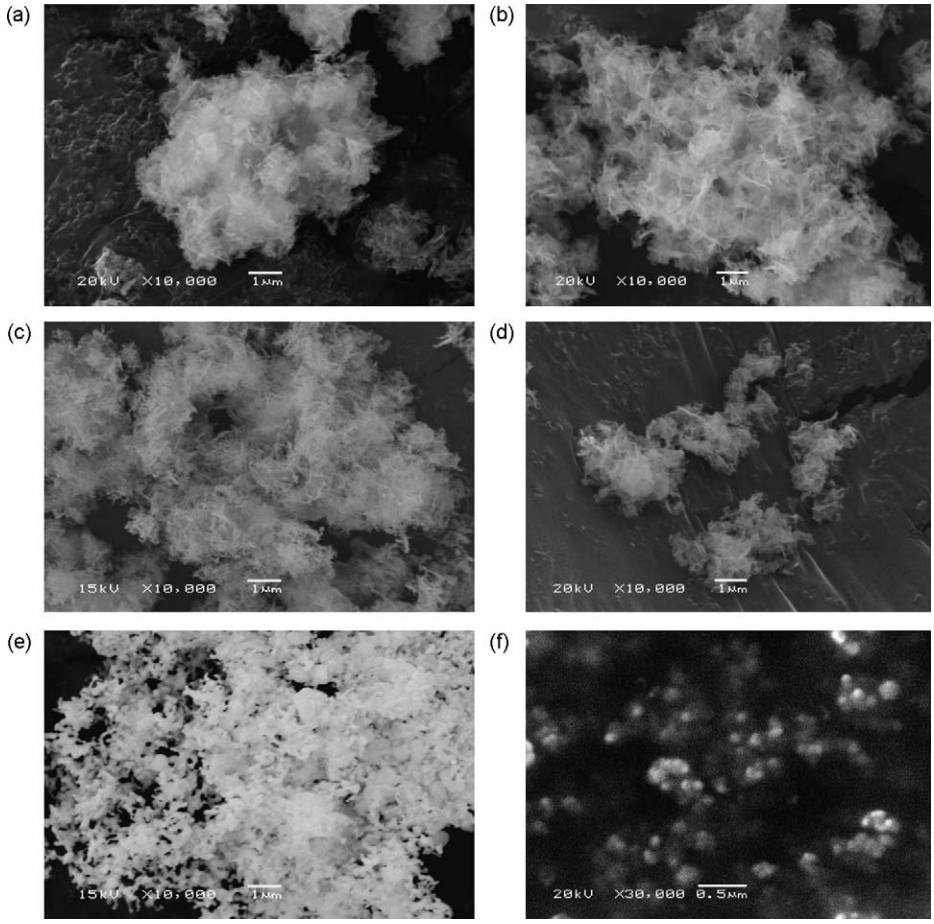

Fig. 7. SEMs of yttria samples obtained at pH 7 and 4 h of aging at 40 °C after calcinations at different temperatures; (a) 500 °C, (b) 600 °C, (c) 700 °C, (d) 800 °C, (e) 900 °C and (f) Y_2O_3 of (d) dispersed in ethanol.

2.3. Characterizations

Phase identification was performed via X-ray diffractometer (XRD) (Model D/MAX2000 Rigaku), using Cu Kα radiation and a scanning speed of $2\theta = 5^\circ$ min^{-1}. Morphology and particle size of the yttria powders were observed using Energy Filtered Transmission Electron Microscope (EF-TEM) (Model omega 912 Carl Zeiss) and SEM (JEOL JSM 6380). To identify the form of precursor, Fourier transformed infra-red spectrometer (FT-IR) (Model Genesis II FT-IR^{TM} Mattson) was used. Finally, to understand thermal behavior, thermogravimetric analysis (TGA) (Model TA2050 TA instruments) was conducted. The particle size in dispersion was measured using particle size analyzer (Zeta Pals, Brookhaven Inst. Co.). Light transmittance was measured using a spectrometer (HP, Agilent 8453).

3. Results and discussion

3.1. Effect of precipitant

Normal striking method where precipitant is added to precursor metal salt solution was adopted and three different precipitants such as NH_4OH, mixture of NH_4OH and $(NH_4)_2CO_3$ and $(NH_4)_2CO_3$ were used. Upon adding precipitant, the solution pH was monitored and shown in Fig. 2. As can be seen in Fig. 2, upon addition of NH_4OH as a precipitant, the pH was rapidly increased and reached plateau at around pH 6.5, indicating the completion of precipitation as $Y(OH)_3$ through reactions (1) and (2). In case of the mixture of NH_4OH and $(NH_4)_2CO_3$ as a precipitant, however, the pH was shortly increased at very initial stage followed by rapid decrease to pH 4.5. It is attributed to the formation of basic yttrium carbonate through the competition between NH_4OH and $(NH_4)_2CO_3$ where OH^- ions are released and the reaction of $(NH_4)_2CO_3$ with Y^{3+} ions takes place to form $Y_2(CO_3)_3$ which subsequently react with OH^- through reactions (3)–(7).

$$NH_4OH \Leftrightarrow NH_4^+ + OH^- \quad (1)$$

$$Y^{3+} + OH^- \Leftrightarrow Y(OH)_3(\downarrow) \quad (2)$$

$$NH_4OH + NH_4HCO_3 \Leftrightarrow (NH_4)_2CO_3 + H_2O \quad (3)$$

$$2Y(NO_3)_3 + 3(NH_4)_2CO_3 \Leftrightarrow Y_2(CO_3)_3 + 6NH_4NO_3 \quad (4)$$

$$2Y(NO_3)_3 + 6NH_4HCO_3 + n{\cdot}H_2O \Leftrightarrow Y_2(CO_3)_3{\cdot}nH_2O + 6NH_4NO_3 + 3CO_2 + 3H_2O \quad (5)$$

$$Y_2(CO_3)_3 + 2OH^- \Leftrightarrow 2Y(OH)CO_3(\downarrow) + CO_3^{2-} \quad (6)$$

$$2Y(OH)CO_3 \rightarrow Y_2O_3 + 2CO_3 + H_2O \quad (7)$$

In case of NH_4HCO_3 as a precipitant, Fig. 2 shows greater decrease in pH through the following reactions of (8)–(10) than of previous case, reaching the completion of precipitation at pH 4.7.

$$NH_4HCO_3 \Leftrightarrow NH_4^+ + HCO_3^- \quad (8)$$

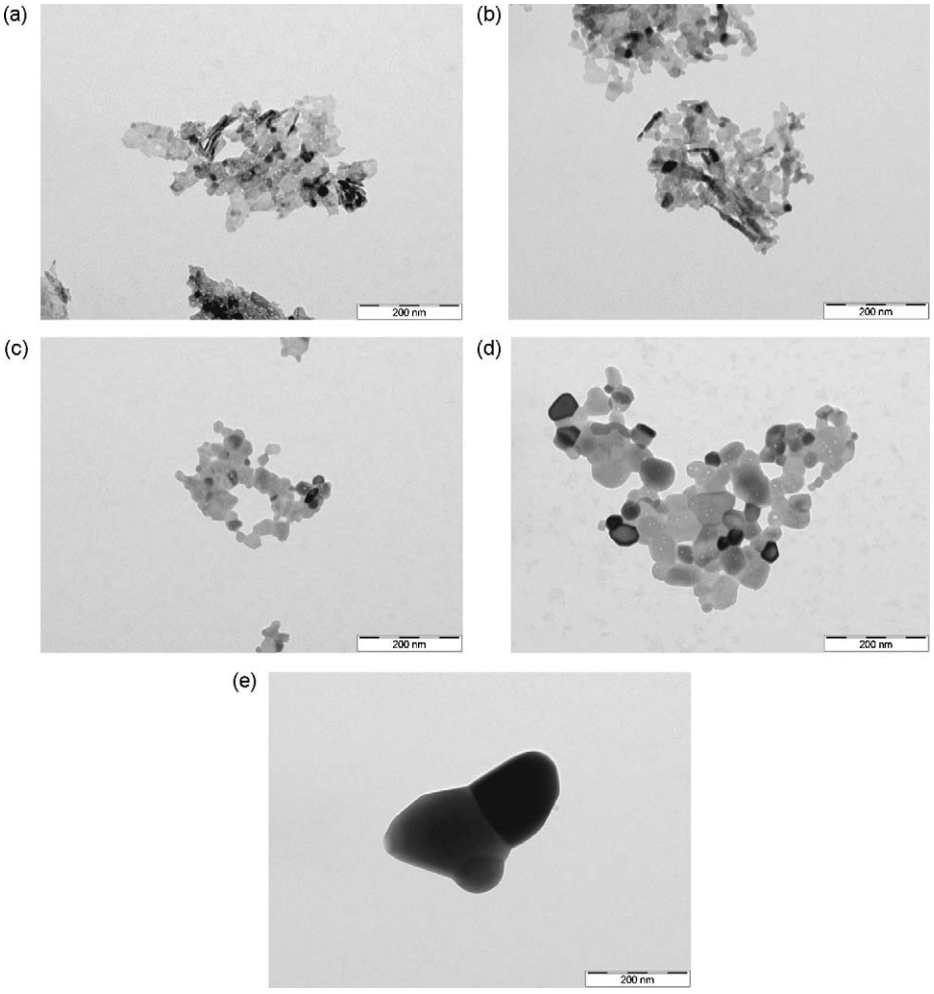

Fig. 8. FETEM of yttria samples obtained at pH 7 and 4 h of aging at 40 °C after calcinations at different temperatures; (a) 500 °C, (b) 600 °C, (c) 700 °C, (d) 800 °C and (e) 900 °C.

$$HCO_3^- \Leftrightarrow H^+ + CO_3^{2-} \quad (9)$$

$$2Y^{3+} + 3CO_3^{2-} \Leftrightarrow Y_2(CO_3)_3(\downarrow) \quad (10)$$

Figs. 3 and 4 show XRD patterns and TEM of yttria nano-powders synthesized at pH of 8 using different precipitants. Each product was calcined at 800 °C for 4 h. Fig. 3 shows that no other phase than yittria has been formed and the characteristic peak of yittria has become narrow and more intense as precipitant was varied from NH_4OH to mixture of NH_4OH and $(NH_4)_2CO_3$ to $(NH_4)_2CO_3$, indicating the acceleration of particle growth. It can be seen in Fig. 4 where TEM image shows the particle growth depending on the type of precipitant. It seems that the particle growth strongly depends on the decrease of pH at the initial stage and thus the rate of precipitation. It is anticipated that the more the pH decreases, the faster the precipitation occurs, finally leading to the formation of larger particle.

Fig. 5 shows IR spectra of the precursors. All the spectra show broad peak at 3400–3500 cm^{-1} and sharp peak at 1640 cm^{-1} corresponding to OH stretching and bending modes, respectively. It is clearly seen that the peak intensity at 1640 cm^{-1} has been gradually weakened as precipitant was changed from NH_4OH to mixture of NH_4OH and $(NH_4)_2CO_3$ to $(NH_4)_2CO_3$. The gradual disappearance of this peak depending on precipitant is attributed to the OH^- dissociated from NH_4OH. A peak at 1515 cm^{-1} was observed only for latter two cases, which refers to C–O stretching bond due to CO_3 group.

3.2. Effect of temperature

Various yttria samples obtained from experiment set B were calcined at different temperature from 500 °C to 900 °C and analyzed by XRD and the XRD patterns are shown in Fig. 6. As can be seen in Fig. 6, the intensity of characteristic peaks was increased with the increase of calcinations temperature, indicating that the higher the calcinations temperature is, the more the crystal growth would take place.

In order to investigate the crystal morphology, the scanning electron micrographs were obtained and shown in Fig. 7. Although the crystal size and morphology cannot be precisely identified from this figure, there seems no significant difference in flake shape of morphology for the samples calcined at 600–800 °C. It is interesting to notice, however that the sample calcined at 900 °C shows crystal growth with spherical shape of particles inter-connected each other. This result is quite consistent with that of XRD where the peak intensity of the sample calcined at 900 °C as shown in Fig. 6 was increased and very sharp. Fig. 7(f) shows the yttria powder corresponding to the sample (d) with ~100 nm which was dispersed in ethanol. Although the agglomeration of yttria particles is significant as shown in Fig. 7(a)–(e), Fig. 7(f) clearly shows that the physically agglomerated yttria particles can be fairly well dispersed in ethanol.

To manifest the effect of calcination temperature on crystal growth, FETEM was taken for the same samples and shown in Fig. 8. It clearly shows the increase in crystal growth with calcination temperature and quite consistent with XRD and SEM.

In order to choose the optimal organic solvent, yttria powder was dispersed in several organic solvents such as MEK (methyl ether ketone), NBA (normal butyl alcohol), EA (ethyl acetate) and IPA (isopropyl alcohol) to choose an optimal solvent which shows the best dispersion and the SEMs are shown in Fig. 9. As can be seen in Fig. 9, IPA shows the most excellent dispersion and it was therefore chosen as an organic solvent.

Once organic solvent was chosen, several dispersants were tested and the result was shown in Fig. 10. The SEM in Fig. 10 shows that phosphoric acid ester was proven to be the best and thus chosen as a dispersant.

Once organic solvent and dispersant were determined, the effects of bead size, rpm and dispersion time on the dispersity were tested and the results are shown in Fig. 11(a)–(c), respectively. As

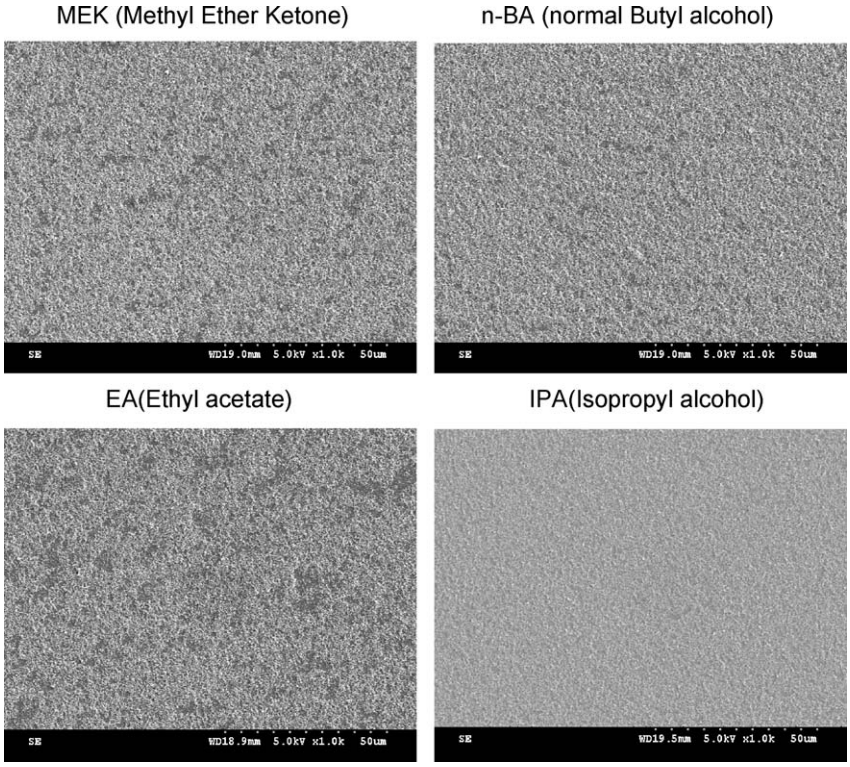

Fig. 9. SEMs of yttria powders dispersed in different organic solvents.

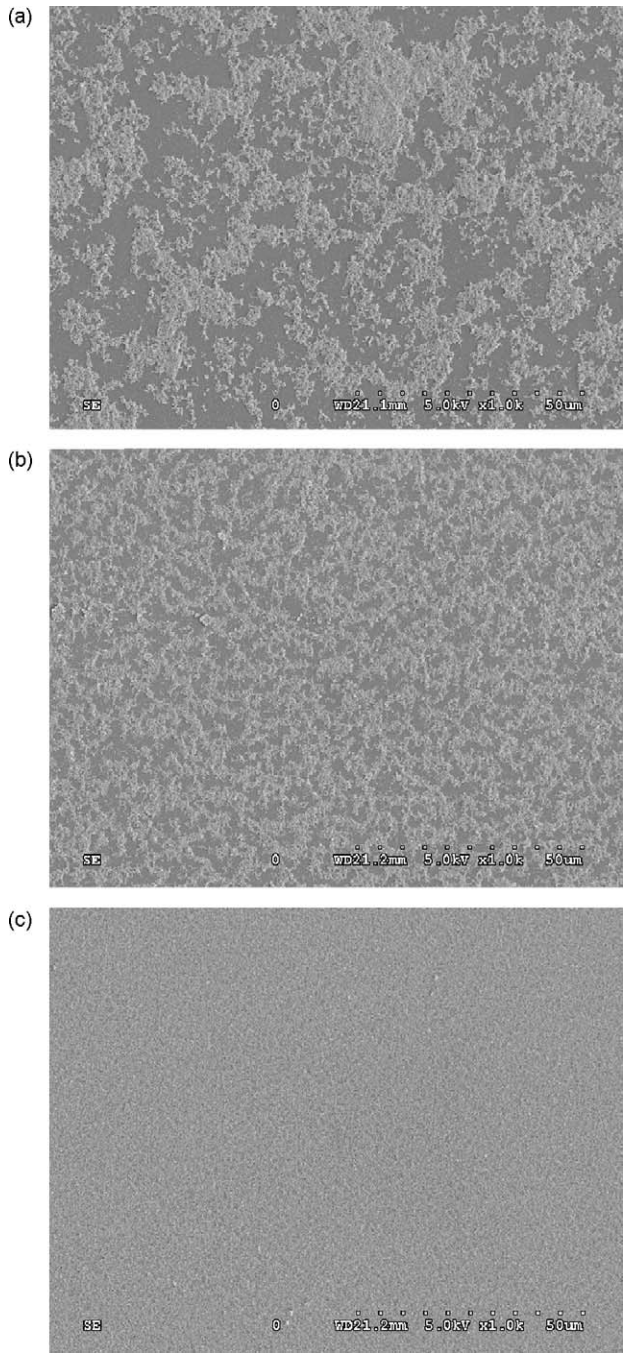

Fig. 10. SEMs of Y_2O_3 powder dispersed in different dispersant system; (a) acrilate co-polymer, (b) alkyl ammonium and (c) phosphoric acid ester.

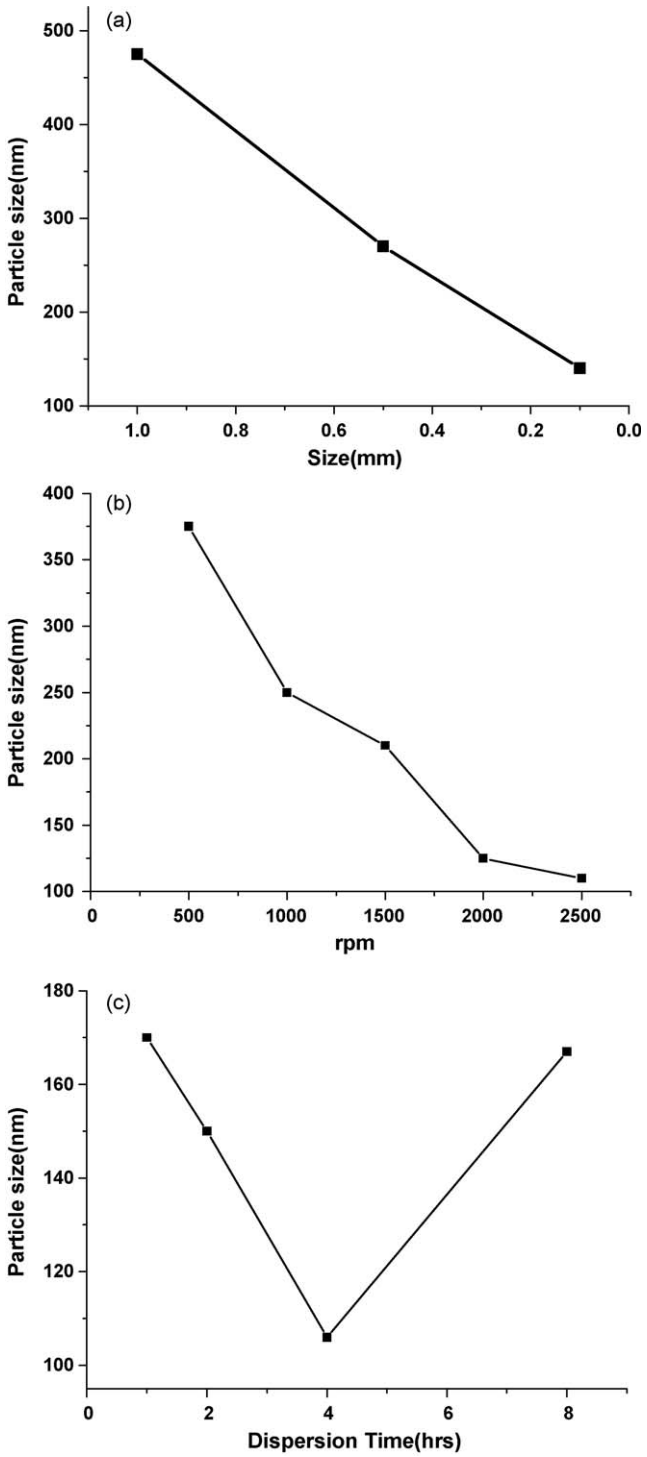

Fig. 11. Dispersed particle sizes with various factors: (a) bead size, (b) rpm and (c) dispersion time.

can be seen in Fig. 11(a) and (b), 0.1 mm bead formed the smallest particle size and 2500 rpm using 0.1 mm of bead yielded the smallest particles dispersed in dispersant. Finally, using these optimum bead and rpm, the dispersion of yttria powder was conducted for various times and the minimum particle size was obtained after 4 h of dispersion as shown in Fig. 11(c). As the dispersion time increased beyond 4 h, however, the particle size dispersed in solution was rather increased due to agglomeration of particles, thus choosing 4 hrs of dispersion time as an optimum.

After the optimal dispersion conditions such as bead size, rpm and dispersion time were determined, yttria powder was dispersed. The particle size and size distribution was measured using IPA and phosphoric acid ester as organic solvent and dispersant, respectively. The average particle size was then observed to be about 114 nm and the size distribution is shown in Fig. 12.

The physical properties of yttria powder were measured and summarized in Table 1. As can be seen in Table 1, the physical properties are highly feasible to apply to BLU.

In order to investigate the coating characteristics of dispersion, the glass slide was dipped into yttria dispersion and the SEM was taken. The SEM is shown in Fig. 13. As can be seen in Fig. 13(a), the coated surface of yttria dispersion is fairly uniform and the cross

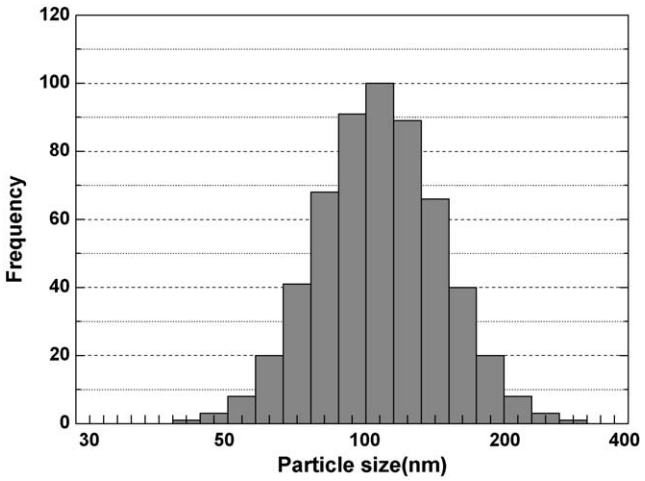

Fig. 12. Particle size distribution of yttria powder.

Table 1
Summary of physical properties of yttria powder.

Specific gravity (25 °C)	Viscosity (25 °C)	%Solid	pH
0.850	2.60	10.25	8.98

sectional view in Fig. 13(b) shows a uniform thickness of about 500 nm. Light transmittance is an important property to evaluate the optical property. Fig. 14 shows the % transmittance over the wavelength ranging from 350 nm to 800 nm for yttria coated glass. Fig. 14 shows that % transmittance was excellent which led to excellent brightness as shown in Fig. 15.

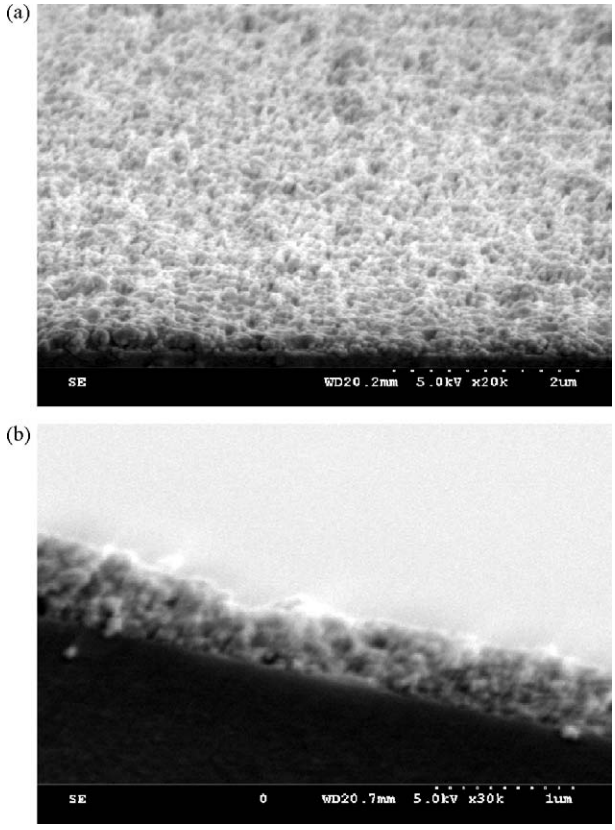

Fig. 13. SEM of yttria dispersion coating layer: (a) plane surface and (b) cross sectional view.

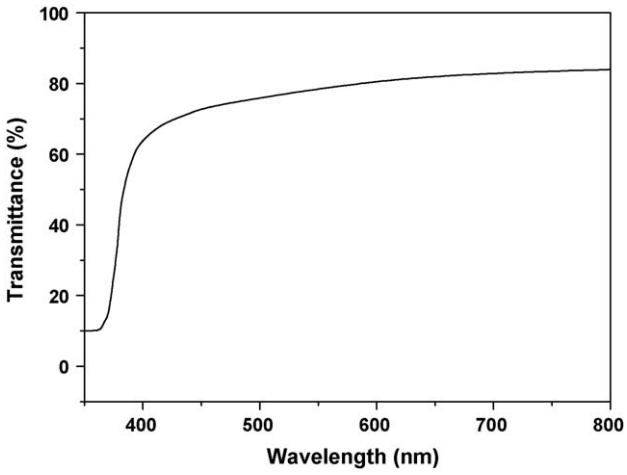

Fig. 14. Optical transmittance spectrum of yttria dispersed in glass slide.

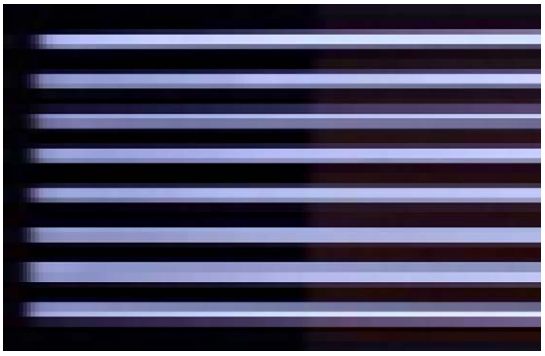

Fig. 15. Brightness test of lamp coated by yttria dispersion obtained in this study.

4. Conclusions

Through this study, several conclusions have been drawn as follows. The size of yttria powder is significantly affected by type of precipitant: that is, depending on the rate of formation of precipitate which controls the solution pH, the crystal growth should have been determined. It is seen that NH_4HCO_3 shows the most significant decrease in pH during the formation of $Y_2(CO_3)_3$. The result shows that yttria powder size depends on the calcination temperature but the agglomeration becomes more significant beyond 800 °C. However, the SEM clearly shows that the agglomerated powder can be fairly well dispersed in ethanol, indicating physical agglomeration. It was also observed that the morphology of yttria powder calcined up o 800 °C shows flake type while beyond 800 °C shows spherical shape interconnected each other.

It was observed that IPA and phosphoric acid ester shows the best performance in dispersion and the average particle size dispersed in this dispersion system was 114 nm. The dispersion of yttria powder obtained can be affected by bead size, rpm and dispersion time.

Finally, % transmittance and brightness test indicates that yttria synthesized by precipitation and dispersed in optimal organic solvent and dispersant is highly feasible for BLU.

Acknowledgement

This study was conducted during the sabbatical year of 2008 in Kon Kuk University.

References

[1] C.K. Gupta, N. Krishnamurthy, Int. Mater. Rev. 37 (1992) 1.
[2] J.H. Sharp, Met. Mater. 6 (1991) 349.
[3] W.E. Rhine, H.K. Bowen, Ceram. Int. 17 (1991) 143.
[4] W.F. Kladnig, Int. J. Mater. Prod. Technol. 7 (3) (1992) 257.
[5] S.M. Sohn, Y.S. Kwon, Y.S. Kim, D.S. Kim, Powder Technol. 142 (2004) 136.
[6] J.Y. Lee, Y.S. Tak, J. Ind. Eng. Chem. 4 (2) (1999) 139.
[7] T. Ikegami, J.G. Ki, T. Mori, J. Am. Ceram. Soc. 85 (7) (2002) 1725.
[8] B.M. Tissue, H.B. Yuan, J. Solid State Chem. 171 (2003) 12.
[9] R. Schmechil, H. Winkle, L. Ziaomao, M. Kennedy, M. Kolbe, A. Benker, M. Winterer, R.A. Fischer, H. Hahn, H. von Seggern, Scr. Mater. 44 (2001) 1213.
[10] P.K. Sharma, M.H. Jilavi, V.K. Varadan, H. Schmidt, J. Phys. Chem. Solids 63 (2002) 171.
[11] Y. Tsukuda, Jpn. Ceram. Soc. Bull. 23 (1988) 456.
[12] C. Greskovich, K.N. Woods, Am. Ceram. Soc. Bull. 52 (1973) 473.